Modeling Laser Imprint for Inertial Confinement Fusion Targets

In inertial confinement fusion (ICF), a spherical shell filled with a DT-gas mixture is compressed to high densities and temperatures to achieve ignition condition.[1] Degradation from spherical symmetry during the implosion, however, limits the achievable compression ratios and could quench the ignition. The main source of such asymmetry is hydrodynamic instabilities (such as the Rayleigh–Taylor and Bell–Plesset instabilities) seeded by both irradiation nonuniformities and impurities in the target materials. In this article we describe a process that generates mass perturbations on an initially uniform target driven by a modulated laser illumination. Such a process is referred to as a "laser imprint." The control of laser imprint is of crucial importance for the successful implosion of direct-drive ICF targets. To evaluate the imprint growth, the following two physical problems must be considered: (1) generation of nonuniformities in ablation pressure due to spatial modulations in a laser intensity, and (2) mass perturbation growth on a target driven by nonuniform ablation pressure. A detailed analysis of the first problem can be found in Refs. 2. The second problem, however, has not been adequately treated in the past. In Ref. 3, for example, perturbation growth was derived by using the Chapman–Jouguet deflagration model. As discussed in Refs. 4, such a model neglects thermal smoothing of perturbations in the conduction zone (a region between the critical surface and ablation front), and in addition, it does not reproduce the main restoring force, which is due to a difference in the dynamic pressure at the peaks and valleys of the front distortion.[5,6] An improved model has been proposed in Ref. 4, where thermal smoothing of the pressure perturbations has been included. At the ablation front, however, the authors used the "Landau–Darrieus" boundary condition that, similar to the result of Ref. 3, neglects the main stabilizing force due to the dynamic overpressure.

The main goal of this article is to give a theoretical description of the hydrodynamic coupling between the pressure perturbation and the ablation-front modulation. The developed theory is relevant to the stability of high-isentrope ($\alpha \geq 2$, where α is the ratio of the pressure at a given density to the Fermi pressure) ICF targets directly driven by a laser pulse that consists of a low-intensity (a few 10^{13} W/cm^2) foot followed by the main drive pulse. During the foot pulse, the ablation pressure created by the mass ablation generates a shock wave that propagates through the shell. Since the laser intensity is constant during the shock transit time, the pressure behind the shock is uniform and the ablation front travels at a constant velocity. Later, as intensity increases during the main pulse (in direct-drive cryogenic target designs the beginning of the main pulse is timed to the first shock breakout of the shell[7]), the shell starts to accelerate and front perturbations η begin to grow because of Rayleigh–Taylor (RT) instability $\eta \sim \eta_0 e^{\gamma_{\mathrm{RT}} t}$, where γ_{RT} is the RT instability growth rate. If the perturbation amplitude becomes too large during the implosion, the shell breaks up, and the ignition condition cannot be reached. To quantify the shell integrity, we introduce an "integrity factor" $\Upsilon = A_{\mathrm{mix}}/\Delta R$, which is defined as a ratio of the mix amplitude (bubble amplitude) A_{mix} to the shell thickness ΔR. The bubble amplitude is taken to be[1] $A_{\mathrm{mix}} = \sqrt{2}\sigma$, where

$$\sigma^2 = \sum_{l,m} \left|\eta_{l,m}(t)\right|^2 \Big/ (4\pi)$$

is the rms sum of the modes, $\eta_{l,m} = \int d\Omega Y^*_{l,m}(\Omega)\, R(\Omega,t)$, $R(\Omega,t)$ is the radius at solid angle Ω and time t, and $Y^*_{l,m}$ is the complex conjugate of the l,m spherical harmonic. The shell remains intact during the implosion if the integrity factor is less than unity ($\Upsilon < 1$ for all time). Simulations performed for direct-drive cryogenic OMEGA and NIF target designs show that to satisfy the condition $\Upsilon < 1$ during the implosion, the integrity factor Υ_0 at the shock breakout time t_{br} must be less than $\Upsilon_0^{\max} = 0.01$. In this article we present a model to estimate $\Upsilon_0^{\mathrm{imp}}$ due to the laser imprint. Such a model sheds some light on physical mechanisms driving the laser-imprint growth. To proceed with our analysis, first we note that during the prepulse, the shell's outer radius R is much larger than the target thickness ΔR, and convergence effects can be neglected. All perturbations are then decomposed in the Fourier space $\eta = \sum_k \eta_k e^{ikx}$, where

$$\eta_k \simeq \eta_{l,m}\sqrt{\frac{(2l+1)}{8\pi}},$$

$k \simeq l/R$ is the wave number, and l is mode number. Since the perturbation amplitude in the linear regime is proportional to the laser nonuniformity, we introduce a normalized amplitude $\eta_{k,\delta I} \equiv \eta_k/(\delta I_k/I_0)$, where δI_k is the Fourier component of the intensity modulation and I_0 is the average intensity. Then, the integrity factor takes the following form:

$$\Upsilon^2 \equiv \Sigma_k\, \Upsilon_k^2 = \Sigma_k \left|\eta_{k,\delta I}(\delta I_k/I_0)/\Delta R\right|^2.$$

Nonuniformity in the laser illumination $\delta I_k/I_0$ can be obtained from the spectrum of the laser speckle on target produced by the distributed phase plates (DPP's). Thus, to estimate the integrity factor, we must calculate an imprint amplitude $\eta_{\rm imp} \equiv \eta_{k,\delta I}/\Delta R$ at the shock breakout time (beginning of the main pulse) $t = t_{\rm br} = \Delta R_0/U_s$, where ΔR_0 is the uncompressed shell thickness and U_s is the shock speed. For strong shocks [when the ratio of the ablation pressure p_a and the initial pressure of the undriven shell p_0 is large $(\Pi \equiv p_a/p_0 >> 1)$] and the ratio of specific heat $\gamma = 5/3$, the shock breakout time is $t_{\rm br} \simeq 2\Delta R/c_s$, where c_s is sound speed of compressed material and $\Delta R \simeq \Delta R_0/4$.

The laser imprint growth is determined by several physical effects. First, as the laser energy is absorbed by the outmost layer of the shell at the beginning of implosion, the shell material heats up, launching a heat wave toward the pellet center. Material behind the heat front expands outward, creating an ablation pressure p_a that induces a shock wave propagating through the shell. Nonuniformities in the intensity across the laser beam cause different parts of the beam to ablate shell material at different rates, generating an ablation-pressure modulation $\tilde{p}_a$ along the ablation front. Since the shock speed U_s scales as a square root of the shock strength Π ($U_s \sim \sqrt{\Pi}$ for $\Pi >> 1$), stronger shocks launched at the peaks of ablation pressure propagate faster than the shocks launched at the pressure valleys. A difference in the shock speed distorts the shock front and creates a perturbed velocity field inside the compressed region. A velocity perturbation at the ablation front, in turn, leads to a linear-in-time front distortion growth $\eta \sim \tilde{v}_x t$, where $\tilde{v}_x \sim \tilde{p}_a U_s/(2p_a)$, and the x axis points in the direction of laser propagation. Note that such a growth is wavelength independent. Then, in order to conserve the tangential component of the fluid velocity, a rippled shock front generates a lateral mass flow from the convex part of the shock front (which protrudes the most into the cold region) into the concave part (Fig. 80.1). A change in density, according to the adiabatic condition $\partial_t \tilde{p} = c_s^2 \partial_t \tilde{\rho}$, leads to a pressure deficiency in the convex part and a pressure excess in the concave part. Since the pressure perturbation at the ablation front is fixed by the laser-beam nonuniformities, the lateral flow creates a negative pressure gradient toward the convex part of the shock front and a positive one toward the concave part. The pressure gradient accelerates fluid elements $\rho d_t^2 \eta = \rho \tilde{a} \sim \partial_x \tilde{p}_a$, leading to an additional perturbation growth $\eta \sim \partial_x \tilde{p}_a/(2\rho)t^2$, where ρ is the compressed density and η is the ablation front amplitude. After the shock front has moved a distance of the order of perturbation wavelength from the ablation front, the latter reaches a steady state (assuming that the ablation pressure modulation is constant in time), and the pressure perturbation in the vicinity of the ablation front obeys Laplace's equation $\partial_x^2 \tilde{p} - k^2 \tilde{p} = 0$. Keeping only a decaying solution of that equation, $\tilde{p} \sim \tilde{p}_a e^{-kx}$, leads to a finite pressure gradient, a perturbed acceleration of the ablation front, $\tilde{a} \sim \partial_x \tilde{p}_a/\rho \simeq k\tilde{p}_a/\rho$, and a quadratic-in-time asymptotic perturbation growth $\eta(kc_s t >> 1) \sim (\tilde{p}_a/\rho)kt^2/2$.

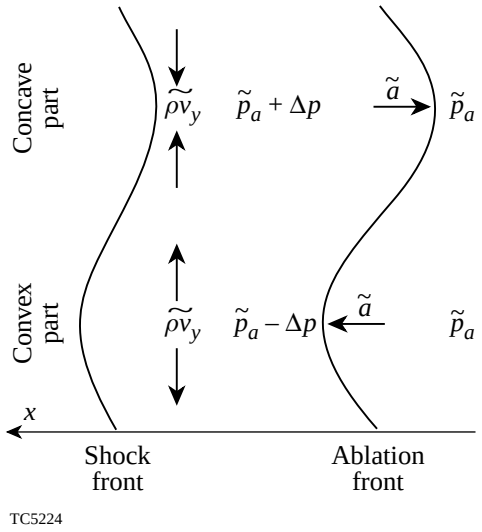

Figure 80.1
Lateral mass flow generated by the rippled shock creates a pressure excess behind the concave part of the shock front and a pressure deficiency behind the convex part.

A rigorous derivation of the perturbation evolution in the "classical" case (constant-in-time ablation-pressure modulation and no mass ablation) is performed by solving the mass, momentum, and energy conservation equations. Such a derivation (to be discussed in detail in a forthcoming paper[8]) yields a result similar to the one obtained above by using a simple physical argument. For strong shocks $\Pi >> 1$ and $\gamma = 5/3$, the

solution is

$$\eta(t) \simeq \frac{\tilde{p}_a}{p_a}\left(0.7\, c_s t + 0.3\, k c_s^2 t^2\right). \quad (1)$$

Note that Eq. (1) can be reproduced by solving a simple second-order differential equation

$$d_t^2 \eta = \tilde{a} = k\frac{\tilde{p}_a}{\gamma p_a} c_s^2 \quad (2)$$

with the initial conditions $\eta(0) = 0$ and $\eta'(0) = 0.7\left(\tilde{p}_a / p_a\right) c_s$. To calculate the imprint amplitude η_{imp}, we assume[2] $p_a \sim I^{2/3}$ and $\delta I_k / I_0 = (3/2)\tilde{p}_a / p_a$, hence

$$\eta_{\text{imp}}^{\text{cl}} \simeq 0.8\, k\Delta R + 0.9 \simeq 0.8\frac{l}{A} + 0.9, \quad (3)$$

where $A = R/\Delta R$ is the shell's in-flight aspect ratio (IFAR). Equation (3) shows that the imprint amplitude of long-wavelength modes ($k\Delta R << 1$ or $l < 15$ for directly driven NIF targets) is wavelength independent; at short wavelengths, however, the imprint amplitude is proportional to the mode number l and inversely proportional to the IFAR. In addition, the imprint amplitude in the classical case does not depend on the laser intensity. Next, we calculate the integrity factor for a direct-drive $\alpha = 3$ NIF target design[7] using η_{imp} in the form of Eq. (3). The amplitudes $\delta I_k / I_0$ can be estimated by using the results of Ref. 9. The calculation yields $\Upsilon_0^{\text{imp}} \simeq 0.2$, which is a factor of 20 larger than the stability threshold $\Upsilon_0^{\max}$. The RT instability seeded by such a perturbation would disrupt the shell during the acceleration phase of implosion and quench the ignition. In direct-drive ICF, however, several physical processes significantly reduce the imprint growth. Next, we consider the main stabilizing mechanisms inherent to laser-driven targets: thermal conduction smoothing and mass ablation.

Thermal Conduction Smoothing

As the heat front (ablation front) propagates into the cold portion of the target, material heats up and expands outward creating a hot plasma corona. The laser light is absorbed in a region (absorption region) where the density of blown-off material is much lower than the compressed shell density. Thus, a finite zone (conduction zone) of hot plasma exists between where the laser energy is deposited and the ablation front. Because of the high temperatures, any pressure perturbations inside such a region are smoothed out by the thermal conduction. The simplest theory[10] predicts that pressure perturbations decay exponentially away from the critical surface ("cloudy-day effect") $\tilde{p} \sim e^{-kx}$; thus, nonuniformities in the ablation pressure are reduced by a factor e^{-kD_c}, where D_c is a distance between the absorption region and the ablation front. More-sophisticated models of thermal smoothing[2] yield similar behavior of the reduction coefficient. To simplify the analysis, the distance D_c is taken to be $D_c \simeq V_c t$; this leads to an exponential decay in the ablation pressure perturbation $\tilde{p}_a \simeq \tilde{p}_a(0) e^{-kV_c t}$. After $t = \left(kV_c\right)^{-1}$, laser nonuniformities with the wave number k decouple from the ablation front, nullifying the k-Fourier component of the perturbed acceleration $\tilde{a}$. The ripple of the ablation front, however, continues to grow due to a finite velocity perturbation

$$\eta\left[t > \left(kV_c\right)^{-1}\right] \sim \tilde{v}_x t.$$

Scaling laws of the perturbation growth can be derived by solving Eq. (2) and substituting $\tilde{p}_a = \tilde{p}_a(0) e^{-kV_c t}$ into its right-hand side:

$$d_t^2 \eta_a = k\frac{\tilde{p}_a(0)}{\gamma p_a} c_s^2 e^{-kV_c t}. \quad (4)$$

The imprint amplitude in this case takes the following form:

$$\eta_{\text{imp}}^{\text{th}} \simeq \frac{0.4\, A}{l}\left(\frac{c_s}{V_c}\right)^2 \left(e^{-\Delta_c} - 1\right) + 0.9 + 0.8\frac{c_s}{V_c}, \quad (5)$$

where $\Delta_c = 2(l/A)V_c/c_s$. Equation (5) shows that for modes with $\Delta_c > 1$ ($l > 10$ for direct-drive NIF targets) thermal smoothing reduces the imprint amplitude by a factor $\eta_{\text{imp}}^{\text{th}} / \eta_{\text{imp}}^{\text{cl}} \sim A/l$.

Mass Ablation

An additional reduction in the imprint growth is due to the mass ablation. The main stabilizing mechanism produced by ablation is the dynamic overpressure or "rocket effect"[5,6] that can be described as follows: Laser-beam nonuniformities create ablation-pressure modulations along the target surface. Such modulations (see discussion earlier in the text) distort the ablation front: front peaks protrude into the hot plasma corona, and the valleys move toward the cold target material. Analysis of Ref. 5 shows that because of high thermal conductivity in the blowoff region, temperature is uniform along the heat (ablation) front. Thus the ablation front's distortion growth slightly increases the temperature gradient at the front peaks and decreases it at the front valleys. An increase in the temperature gradient leads to an additional heat flow that speeds up the

heat front and increases the velocity of the blown-off material $V_{\rm bl}$. Higher blowoff ("exhaust") velocity creates an excess in the dynamic pressure ("rocket effect" increases). At the perturbation valleys, the picture is reversed: a reduction in the temperature gradient decreases the ablation and blowoff velocities, thus the dynamic pressure and the rocket effect are also reduced. We can conclude that the modulation in the dynamic pressure created by the thermal conduction reduces the perturbation growth and ultimately stabilizes the growth completely. Calculations[5] show that the amplitude of the dynamic pressure is proportional to the front distortion $\tilde{p}_d = \dot{m} V_{\rm bl} k\eta$. Hence, perturbations reach a saturation value $\eta_{\rm sat}$ when the dynamic-pressure modulation balances the ablation-pressure modulation $\tilde{p}_a \sim \dot{m} V_{\rm bl} k\eta_{\rm sat}$, where $\dot{m} = \rho V$ is the mass ablation rate. Next, to perform a quantitative stability analysis, we solve the system of conservation equations assuming a sharp interface at the ablation front and a constant-in-time ablation-pressure modulation $\tilde{p}_a$.[8] Skipping lengthy calculations, we report a final formula for the asymptotic behavior ($kc_s t >> 1$) of the front-surface perturbations in the case of strong shocks $\Pi >> 1$ and $\gamma = 5/3$:

$$\frac{\eta(t)}{\tilde{p}_a/(\gamma p_a)} \simeq \frac{kc_s^2}{\omega^2}(1 - D\cos\omega t) + \frac{c_s}{\omega}\left(1.2 - \frac{2c_s}{V_{\rm bl}}\right) D\sin\omega t + \eta_v(t), \qquad (6)$$

where $D = e^{-2kV_a t}$, V_a and $V_{\rm bl}$ are the ablation and blowoff velocities, respectively, and $\omega = k\sqrt{V_a V_{\rm bl}}$. The last term η_v is due to the vorticity convection from the shock toward the ablation front:

$$\eta_v = \frac{2c_s}{kV_{\rm bl}}\left[e^{kV_a t}\int_{kV_a t}^{\infty} e^{-\tau}\Omega(2\tau)d\tau - 1.2\ D\cos\omega t\right],$$

where

$$\Omega = i(\nabla \times \mathbf{v})_z \big/ (kc_s \tilde{p}_a/\gamma p_a) \simeq 3J_0(\tau) - 2J_4(\tau)$$

is the normalized vorticity and $J_n(\tau)$ is the Bessel function. Equation (6) shows that the front perturbation grows according to Eq. (1) until the distortion amplitude becomes big enough and the dynamic overpressure balances the ablation-pressure perturbation. After that time, the ablation front oscillates around an average amplitude $<\eta> = \eta_{\rm sat}$. In addition, the difference in the ablation velocity at the distortion peaks and valleys and also the vorticity convection from the ablation front damp the perturbation amplitude [factor $e^{-2kV_a t}$ in Eq. (6)].

The next step is to combine effects of the mass ablation and thermal smoothing. An analytical solution of conservation equations in this case has a very lengthy form.[8] We omit a rigorous derivation of such a solution in this article, however, noting that the essential physics of the imprint growth reduction can be described by an approximate solution derived from Eq. (2) with the following modifications: To take into account the mass ablation effects, first, we add to the left-hand side of Eq. (2) the stabilizing term due to the dynamic overpressure (rocket effect) $\omega^2\eta$, and then, the damping term $4kV_a d_t\eta$, which is due to the difference in the mass ablation rate at the front peaks and valleys and also to the vorticity convection downstream from the ablation front. Thermal smoothing of the pressure perturbations inside the conduction zone is included, the same way as in Eq. (4), by introducing a reduction factor $e^{-kV_c t}$ into the right-hand side of Eq. (2). As a result, the equation describing the evolution of the ablation-front distortion takes the following form:

$$d_t^2\eta + 4kV_a d_t\eta + \omega^2\eta = k\frac{\tilde{p}_a(0)}{\gamma p_a}c_s^2 e^{-kV_c t}. \qquad (7)$$

Observe that neglecting the reduction factor $e^{-kV_c t}$ yields solution (6) (except for the vorticity term η_v). Substituting the solution of Eq. (7) into the definition of the imprint amplitude gives

$$\eta_{\rm imp}^{\rm abl} \simeq 0.4\frac{A}{l}\hat{\eta}\left(e^{-\Delta_c} - e^{-2\Delta_a}\cos\Delta_{\rm bl}\right) + \frac{e^{-2\Delta_a}}{\Delta_{\rm bl}}\left(0.9 + 0.8\frac{V_c}{c_s}\hat{\eta}\right)\sin\Delta_{\rm bl} + \eta_v^{\rm imp}, \qquad (8)$$

where

$$\hat{\eta} = c_s^2/\left(V_a V_{\rm bl} + V_c^2\right),$$

$$\Delta_a = 2(l/A)V_a/c_s,$$

$$\Delta_{\rm bl} = 2(l/A)\sqrt{V_a V_{\rm bl}}/c_s,$$

and

$$\eta_v^{\text{imp}} = 0.8\left(A/l\right)\left(c_s/V_{\text{bl}}\right)e^{\Delta_a} \times \int_{\Delta_a}^{\infty} e^{-\tau}\Omega(2\tau)\,d\tau - 1.2e^{-2\Delta_a}\cos\Delta_{\text{bl}}.$$

Equation (8) shows that in the presence of the mass ablation, the imprint amplitude has an oscillatory dependence on the mode number. For modes with $\Delta_a < 1$, the oscillation period and amplitude are determined by the velocity and acceleration perturbation growth reduced by the dynamic overpressure and the mass ablation [the first two terms in Eq. (8)]. For modes with $\Delta_a > 1$, the acceleration and velocity perturbations deposited at the ablation front are damped by the mass ablation [factor e^{-2kV_at} in Eq. (6)], and the behavior of such modes are determined by the vorticity convection from the shock front [the last term in Eq. (8)]. Figure 80.2 shows a comparison of the imprint amplitude calculated for conditions specified in Ref. 7 with and without stabilizing effects. Observe a significant reduction in the imprint growth due to the thermal smoothing and the mass ablation. To apply Eq. (8) to the ICF target designs, the blowoff velocity is taken to be[6,11]

$$V_{\text{bl}} = V_a\Big/\left[\mu(\nu)\left(kL_0\right)^{1/\nu}\right],$$

where ν is the power index for thermal conduction, L_0 is the characteristic thickness of the ablation front,

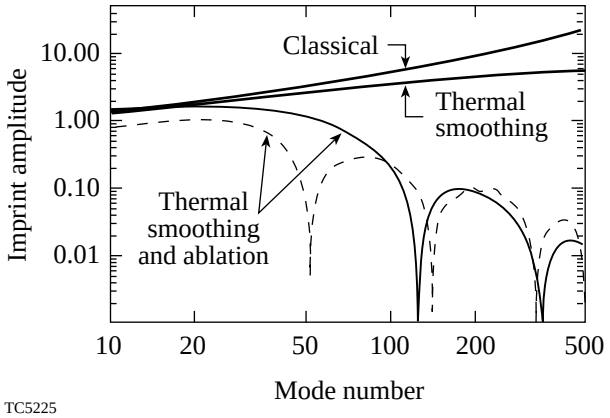

Figure 80.2
Plot of imprint amplitude versus mode number calculated using Eqs. (3), (5), and (8) (solid lines) and 2-D *ORCHID* simulation (dashed line) for a direct-drive, "all-DT," $\alpha = 3$, NIF target design.

$$\mu = \left(2/\nu\right)^{1/\nu}\Big/\Gamma\left(1+1/\nu\right) + 0.12/\nu^2,$$

and $\Gamma(x)$ is the gamma function. The parameters L_0 and ν are obtained by using the fitting procedure described in Ref. 11. For a direct-drive, "all-DT," $\alpha = 3$, NIF cryogenic target design,[7] the 1-D numerical simulations and the fitting procedure give $V_a = 2.5\ \mu$m/ns, $V_c \simeq 30\ \mu$m/ns, $c_s \simeq 37\ \mu$m/ns, $L_0 \simeq 0.03\ \mu$m, and $\nu \simeq 2$. The imprint efficiency calculated by using Eqs. (3), (5), and (8) is plotted in Fig. 80.2 (solid line). For comparison, the results of the 2-D *ORCHID*[12] simulations of single-wavelength imprint amplitudes (dashed line) are shown on the same plot with the model prediction. Observe that the developed model accurately reproduces the oscillatory behavior of the imprint growth. Next, using Eq. (8), the integrity factor is calculated to be $\Upsilon_0^{\text{imp}} = 1.2\times10^{-2}$. Since the outer-surface roughness and also the perturbation "feedout" from the inner surface[13] make an additional contribution to the rms nonuniformity, the total integrity factor is expected to exceed the stability threshold $\Upsilon_0^{\max}$, thus an additional reduction in the imprint amplitude is required for a successful implosion. A significant improvement in beam uniformity has been made in recent years by introducing SSD[14] (smoothing by spectral dispersion) and ISI[15] (induced spatial incoherence) smoothing techniques. To include the effect of SSD in our simulations, the intensity nonuniformities have been reduced by factor

$$\sqrt{t_c/\left(t_c + 4t\right)}$$

that gives on average a reduction in rms nonuniformity

$$\sigma = \sqrt{t_c/t_{\text{avg}}}\,\sigma_0,$$

where the coherence time is taken to be[14]

$$t_c = \left[\Delta\nu\sin\left(k\delta/2\right)\right]^{-1},$$

$\Delta\nu$ is the bandwidth, t_{avg} is the averaging time, and δ is the speckle size. Simulations show that using the 2-D SSD smoothing technique with 1-THz laser bandwidth reduces the integrity factor to $\Upsilon_0^{\text{imp}} = 10^{-3}$, which is a factor of 10 lower than the threshold Υ_0.

In summary, a model describing the evolution of the laser imprint was developed. The model shows that the imprint growth is determined by the velocity and acceleration pertur-

bations generated by the laser-beam nonuniformities. Thermal smoothing inside a hot plasma corona suppresses only the acceleration perturbation, while the mass ablation suppresses both velocity and acceleration perturbations. The model predicts that a direct-drive cryogenic NIF target will remain intact during the implosion when the laser is smoothed with 1-THz SSD used in current direct-drive target designs.

ACKNOWLEDGMENT

This work was supported by the U.S. Department of Energy Office of Inertial Confinement Fusion under Cooperative Agreement No. DE-FC03-92SF19460, the University of Rochester, and the New York State Energy Research and Development Authority. The support of DOE does not constitute an endorsement by DOE of the views expressed in this article.

REFERENCES

1. J. D. Lindl, *Inertial Confinement Fusion: The Quest for Ignition and Energy Gain Using Indirect Drive* (Springer-Verlag, New York, 1998).

2. J. Sanz *et al.*, Phys. Fluids **31**, 2320 (1988); W. M. Manheimer, D. G. Colombant, and J. H. Gardner, Phys. Fluids **25**, 1644 (1982).

3. R. Ishizaki and K. Nishihara, Phys. Rev. Lett. **78**, 1920 (1997).

4. R. J. Taylor *et al.*, Phys. Rev. Lett. **79**, 1861 (1997); A. L. Velikovich *et al.*, Phys. Plasmas **5**, 1491 (1998).

5. J. Sanz, Phys. Rev. E **53**, 4026 (1996); V. N. Goncharov, R. Betti, R. L. McCrory, P. Sorotokin, and C. P. Verdon, Phys. Plasmas **3**, 1402 (1996); A. R. Piriz, J. Sanz, and L. F. Ibanez, Phys. Plasmas **4**, 1117 (1997).

6. V. N. Goncharov, Phys. Rev. Lett. **82**, 2091 (1999).

7. S. V. Weber, S. G. Glendinning, D. H. Kalantar, M. H. Key, B. A. Remington, J. E. Rothenberg, E. Wolfrum, C. P. Verdon, and J. P. Knauer, Phys. Plasmas **4**, 1978 (1997); R. P. J. Town, F. J. Marshall, J. A. Delettrez, R. Epstein, P. W. McKenty, D. D. Meyerhofer, P. B. Radha, S. Skupsky, and C. Stoeckl, Bull. Am. Phys. Soc. **43**, 1666 (1998).

8. V. N. Goncharov, R. Betti, J. A. Delettrez, P. W. McKenty, S. Skupsky, and R. P. J. Town, "Stability Analysis of Directly Driven OMEGA and NIF Targets," to be submitted to Physics of Plasmas.

9. R. Epstein, J. Appl. Phys. **82**, 2123 (1997).

10. K. A. Brueckner and S. Jorna, Rev. Mod. Phys. **46**, 325 (1974); S. E. Bodner, J. Fusion Energy **1**, 221 (1981).

11. R. Betti, V. N. Goncharov, R. L. McCrory, and C. P. Verdon, Phys. Plasmas **5**, 1446 (1998).

12. R. L. McCrory and C. P. Verdon, in *Computer Applications in Plasma Science and Engineering*, edited by A. T. Drobot (Springer-Verlag, New York, 1991).

13. R. Betti, V. Lobatchev, and R. L. McCrory, Phys. Rev. Lett. **81**, 5560 (1998).

14. S. Skupsky, R. W. Short, T. Kessler, R. S. Craxton, S. Letzring, and J. M. Soures, J. Appl. Phys. **66**, 3456 (1989); S. Skupsky and R. S. Craxton, Phys. Plasmas **6**, 2157 (1999).

15. R. H. Lehmberg, A. J. Schmitt, and S. E. Bodner, J. Appl. Phys. **62**, 2680 (1987).